III

Publication III

P. Ahonen, D. J. Schiffrin, J. Paprotny and K. Kontturi, Optical switching of coupled plasmons of Ag-nanoparticles by photoisomerisation of an azobenzene ligand, *Physical Chemistry Chemical Physics*, 2007, **9**(5), 651-658.

Optical switching of coupled plasmons of Ag-nanoparticles by photoisomerisation of an azobenzene ligand†

Päivi Ahonen,[a] David J. Schiffrin,[b] Jerzy Paprotny[b] and Kyösti Kontturi*[a]

Received 20th October 2006, Accepted 23rd November 2006
First published as an Advance Article on the web 11th December 2006
DOI: 10.1039/b615309g

The optical switching of coupled plasmons of silver nanoparticles derivatised with a photoisomerisable azobenzene ligand is presented. It is shown that nanoparticle clusters, linked with an azobenzene dithiol molecule, display switchable optical properties. The photoisomerisation of the linker molecule was used to vary the separation between nanoparticles, which was monitored by changes in the UV-Vis-spectra of the plasmon band of adjacent nanoparticles. A red-shift due to the appearance of a coupled longitudinal plasmon band was observed resulting from the formation of nanoparticle clusters. The maximum absorbance wavelength of this secondary plasmon band was altered by isomerisation of the linker and the spectral changes observed were in good agreement with theory and earlier measurements for gold. Evidence of energy transfer between a nanoparticle and an azobenzene terminated monothiol attached to it was also observed in the UV-Vis spectra.

Introduction

Monolayer protected clusters (MPC) are of great interest for the possibilities in the construction of nanoscale devices by self-assembly techniques.[1–4] Although light offers an attractive trigger for external control of molecular switches, only a limited number of reports on metal nanoparticles modified with photoactive chromophores have been published.[5–10] Azobenzene derivatives are interesting for this purpose because of their reversible *trans*/*cis* photoisomerisation. Although this has been known for a long time, the excitation mechanism and optical properties of the azobenzene chromophore are still under investigation.[11,12] The azobenzene group is isomerised from the more stable *trans* to the *cis* ground state by UV light of 366 nm and back to the *trans* conformer with 436 nm radiation.[13] The photoswitchable azobenzene moiety has been utilised in the past for controlling the properties of functional polymeric materials[14] and for novel applications such as data storage[15,16] and self-assembling systems.[17,18]

Recently, there has been a considerable interest in the properties of azobenzene terminated molecules in self-assembled monolayers on both planar surfaces[19] and on monolayer-protected clusters.[20] Both photochemical and electrochemical reactivity of these interfacial layers have been studied. Photoactivity is strongly affected by the packing density in the monolayers.[6,13,21] For instance, close packing inhibits photoisomerisation in layers assembled on planar substrates, while in mixed monolayers on planar gold surfaces and at nanocluster surfaces, where azobenzene moieties are separated from each other by spacer molecules, the increased free space allows photoisomerisation to occur.[13]

The coupling of optical plasmons in nanoparticles joined by bifunctional linkers depends critically on the interparticle distance.[1,22–29] In the present study a bifunctional linker incorporating an azobenzene functionality was used to link colloidal silver MPCs in solution, since it was of interest to investigate if the optical response of coupled clusters could be controlled by the photoisomerisation reaction. In this case, isomerisation of the linker molecule could be used to alter the longitudinal coupled plasmons of linked nanoparticles and hence explore the changes in optical properties brought about by changing the interparticle distance in optically responsive nanostructures.

Silver nanoparticles and azobenzene were chosen because of the overlap of the nanoparticles' plasmon band with the absorbance bands of azobenzene. The plasmon band of silver MPCs is typically near 440 nm, which also corresponds to the $n \rightarrow \pi^*$ transition of the N=N bond in azobenzene.[12] The matching energy levels of the latter with the silver nanoparticle plasmon band could enable energy transfer between the two species when azobenzene is brought close to the nanoparticle surface. Photoisomerisation of nanoparticles capped with azobenzene-terminated ligands has been previously studied by Evans *et al.*,[13] but the isomerisation yield was very low because of the tight packing of the ligands. In the present work, a low surface coverage of azobenzene was achieved by a thiol exchange-reaction.[28] It was expected that this would provide enough free space for isomerisation to take place.

[a] *Laboratory of Physical Chemistry and Electrochemistry, Helsinki University of Technology, P.O. Box 6100, FIN-02015 HUT, Finland. E-mail: kontturi@cc.hut.fi; Fax: +358-9-451 2580; Tel: +358-9-451 2572*
[b] *Centre for Nanoscale Science, Chemistry Department, University of Liverpool, UK L69 7ZD. E-mail: d.j.schiffrin@liv.ac.uk; Fax: +44-151-794-3588; Tel: +44-151-794-3574*

† Electronic supplementary information (ESI) available: Synthesis of azobenzene derivative. See DOI: 10.1039/b615309g

Experimental

Chemicals

Silver nitrate ($AgNO_3$, Premion®, Alfa Aesar), n-tetraoctyl ammonium bromide (TOABr, 98 + %, Alfa Aesar), sodium borohydride ($NaBH_4$, Merck), 1-dodecane thiol (98%, Lancaster) and ammonium hydroxide (NH_4OH, 99.99 + %, Aldrich) were used as received. Toluene (p.a., Riedel de Haën), acetone (p.a., Fluka) and methanol (p.a., Fluka) were used without further purification.

Synthesis of monolayer protected silver nanoparticles

The synthesis of silver nanoparticles was performed by a two-phase method adapted from the literature.[30] 0.2625 g of silver nitrate was dissolved in 100 mL of Milli-Q® water and silver ions were then transferred into the organic phase with the aid of a molar excess of n-tetraoctyl ammonium bromide (TOABr, 2.5 g in 15 mL of toluene) as the phase transfer reagent. The phases were separated after 2.5 h of stirring and dodecane thiol was added to the organic phase, which was then stirred for approximately 15 min. The molar ratio between thiol and silver was 5 : 3. Sodium borohydride was used as the reducing agent. A tenfold excess of sodium borohydride in 75 mL of water was added into the reaction flask rapidly. The reaction was allowed to proceed further for 1.5–2 h. The solvent was removed in a rotary evaporator after reduction. The nanoparticles were precipitated with 80 mL of acetone at −18 °C and separated by centrifugation, redissolved in a small volume of toluene and precipitated again with 50 mL of acetone. This cleaning procedure was repeated three times. The silver nanoparticle solutions were protected from light during the whole synthesis. Nanoparticles of 3.7 ± 1.6 nm diameter were used in the present work. The particles showed a plasmon band near 460 nm in toluene. A TEM-micrograph and the size distribution of the particles is shown in Fig. 1. The position of the plasmon band for silver nanoclusters with a rather wide size distribution have been previously discussed by Oliveira *et al.*[31]

Synthesis of the azobenzene derivatives

Two compounds were employed, AZO1 and AZO2 (Fig. 2). AZO2 was prepared as the corresponding thioacetyl derivative acetyl AZO2 and deprotected before use. The details of the several steps syntheses are given as ESI.†

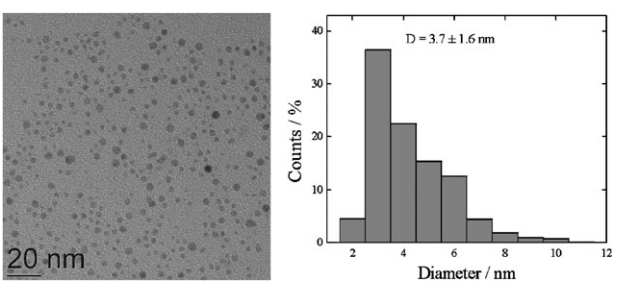

Fig. 1 An example of a TEM-micrograph of the nanoparticles used in the experiments. Inset: Size distribution of the nanoparticles; the average size of the particles was 3.7 nm.

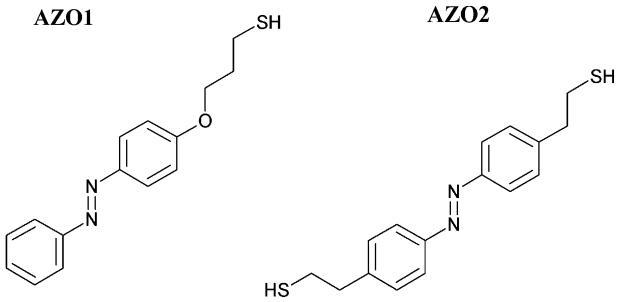

Fig. 2 Azobenzene derivatives used in the experiments.

Synthesis of azobenzene functionalised nanoparticles

The nanoparticles were functionalised by a thiol exchange reaction.[28] 2.7 mg of AZO1 was added to 15 mL of silver MPCs dissolved in toluene (total concentration of silver 0.71 mM). The solution was stirred gently for 5 d. 1 mL samples of the reaction solution were diluted with methanol and filtered in a centrifugal filtration unit (Microsep 30 kDa Omega, Pall Life Siences). The absence of free azobenzene thiol in solution was ascertained by measuring the UV-Vis-spectrum of the filtrate (not shown). Washing was continued until the absorbance peaks of azobenzene could not be observed.

Transmission electron microscopy (TEM)

The nanoparticle size distribution was measured by TEM using a Tecnai 12 instrument operating at a 120 kV accelerating voltage. The samples were prepared by placing a drop of nanoparticles dispersed in toluene on formvar/carbon-coated copper grids (Electron Microscopy Sciences). The grids were dried in air. Size analysis was carried out using ImageJ software.[32]

Photoisomerisation of AZO2

Photoisomerisation of AZO2 was studied by irradiating a sample of a 35 μM toluene solution with light of specific wavelengths. The photoisomerisation was carried out after deprotection of the thiol groups (see below), thus this solution contained small amounts of acetone and methanol. The light source was a 300 W Xe-lamp (Oriel 6259) and the wavelength was selected with a monochromator (Oriel MS257). Isomerisation from the *trans* to the *cis* conformer was achieved by irradiation at 366 nm. The more stable *trans* conformer was restored by irradiation with 436 nm light (see Fig. 3).

Photoisomerisation of AZO1 functionalised nanoparticles

The isomerisation of AZO1 chemically bound to the surface of the nanoparticles was studied by irradiation at 366 and 436 nm. Each irradiation step was 10 min long and the cycle was repeated several times (see Fig. 4).

Formation of AZO2-linked nanoparticle assemblies

The formation of dithiol-linked nanoparticle assemblies was studied *in situ* by UV-Vis spectroscopy. An acetyl-protected azobenzene dithiol, acetyl AZO2, was used as the linker precursor in these experiments. Linking of nanoparticles by

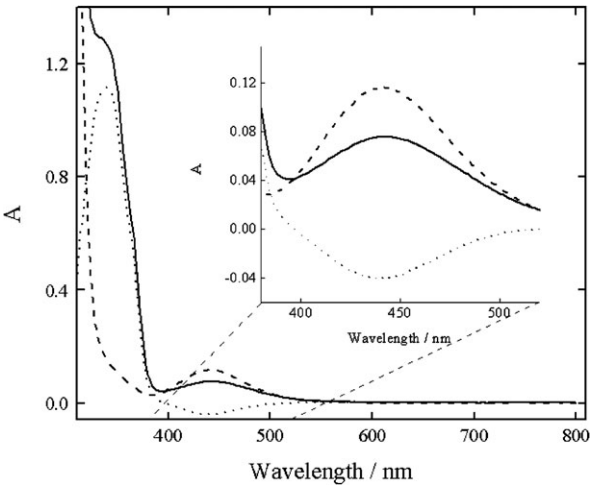

Fig. 3 Absorption spectrum of the *trans* (solid line) and the *cis* conformers (dashed line) of AZO2. The dotted line is the difference between the two spectra. The concentration of AZO2 is 35 μM. Inset: Details of the spectra.

acetyl AZO2 was not observed without removal of the acetyl protection since the UV-Vis spectrum showed no broadening or shift of the plasmon band of the nanoparticles in the presence of the protected molecule. Deprotection was carried out with NH_4OH, as described in the literature.[33] 1.5 mg of the protected azobenzene derivative was first dissolved in a mixture of acetone (5 mL) and methanol (5 mL) and then 0.7 mL of concentrated NH_4OH dissolved in 6.3 mL methanol was added. Such a mixture of solvents was used to prevent separation of phases during deprotection of acetyl AZO2- by aqueous NH_4OH. After 15 min of incubation, the solution was ready to use. Two different preparations of the AZO2-linked nanoparticles were used in the measurements. In the first one, the linker molecule was initially present as the *trans* conformer and in the second one, it was isomerised to the *cis*-form before addition of the nanoparticles. In these experiments, a silver : dithiol ratio of 4.6 was used. In the second experiment, a silver : dithiol ratio of 1.8 was employed. The samples were prepared as follows: 0.5 mL of MPCs in toluene (total concentration of silver 0.71 mM) was added to 2.2 mL of 35 μM AZO2 to obtain a molar ratio of 4.6. For the experiment with a molar ratio of 1.8, 2.5 ml of 77 μM AZO2 was used instead.

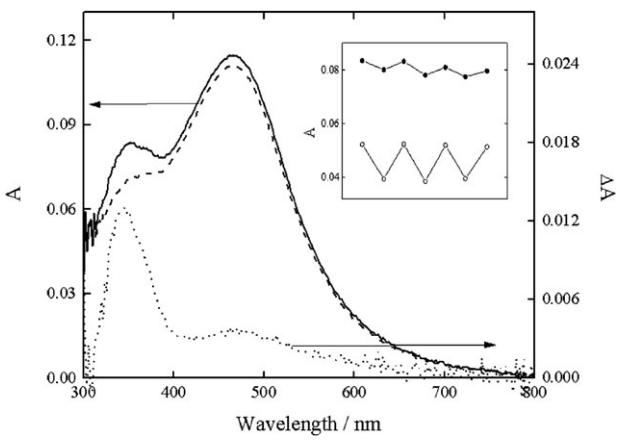

Fig. 4 Spectra of silver nanoparticles functionalised with the *trans* (solid line) and the *cis* conformers (dashed line) of AZO1. The dotted line is the difference between these spectra. Inset: Absorbance at 350 nm (white dots) and 464 nm (black dots) during several *cis–trans* isomerisation cycles.

At the beginning of the experiments, the AZO2 solution was isomerised to the *trans* conformer with 436 nm light or to the *cis* conformer with 366 nm UV light. The spectrum of this solution was monitored and when no further changes were observed, the solution of silver nanoparticles in toluene was added. When the linker was initially in the *cis*-form, the irradiation at 366 nm was continued after the addition of the nanoparticles until the spectrum showed no more changes. After the formation of *cis* AZO2 linked nanoparticles, the azobenzene group was isomerised to the *trans* conformer with 436 nm light. The total concentration of silver in the solutions was determined by ICP-AES (Varian Liberty). The nanoparticle assemblies did not precipitate from solution.

Results and discussion

Isomerisation of Ag nanoparticles capped with AZO1

The UV-spectra of the azobenzene derivatives show two characteristic peaks at 338 and 438 nm (Fig. 3). As previously reported for the parent azobenzene,[11] these derivatives could be photoisomerised repeatedly between the *cis* and *trans* conformations with 366 and 436 nm light, respectively. The *trans* isomer displays a larger absorbance than the *cis* conformer at 338 mm and a lower absorbance, a negative absorbance change on isomerisation, at 438 mm. These spectral changes were reversible. The rise of absorbance that can be observed below 320 nm is due to the small amount of acetone in the solution (see Experimental section).[34]

Fig. 4 shows the changes in the UV-Vis spectrum of silver nanoparticles functionalised with AZO1 resulting from the isomerisation of the attached ligand. The spectra show the characteristic strong surface plasmon band for silver nanoparticles and the spectral changes brought about by isomerisation of the ligand are superimposed to this band. When the azobenzene group was isomerised to the *cis* conformer, the absorbance band corresponding to the $\pi \rightarrow \pi^*$ transition at 348 nm decreased, as in the case of free azobenzene. In contrast with the results obtained with the free azobenzene derivative AZO2 in solution, however, for AZO1 bound to the nanoparticles, the intensity of the absorbance at 444 nm decreased instead of the increase noted in Fig. 3. This wavelength corresponds both to that of the plasmon band and of the $n \rightarrow \pi^*$ transition of the azobenzene group. Thus, if there were no specific interactions between the metal core and the ligand, a decrease in absorbance, as noted in Fig. 3 for the free azobenzene, would have been expected from their combination, instead of the observed increase.

The increased absorbance at 464 nm above the individual contributions could imply that the chromophore attached to a nanoparticle, might absorb energy and transfer it as an excitation to the plasmon band *i.e.*, it could be acting as an antenna. Details of the difference in absorbance observed

between the initial *trans* and the *cis* spectrum in the 400–500 nm region are shown in Fig. 4.

The enhancement of absorbance and fluorescence for molecules close to metal surfaces and nanoparticles has been known for a long time.[35–37] These effects are due to strong interactions of chromophores with surface plasmons, in particular when the absorption bands have frequencies close to each other.[37] A complete understanding of these effects is still incomplete but recent developments in experimental techniques have allowed the study of the enhancement of absorbance resulting form the above interactions.[35] An example of the large estimated absorbance enhancement factors that can be observed, of between 70 and 400, has been calculated for octaethyl porphyrin near nanotextured silver surfaces.[38] Although enhanced absorbance will depend strongly on distance and, in particular, chromophore orientation with respect to the nanoparticle surface, these effects can easily account for the observed differences in intensity of the absorption band of the azobenzene moiety.

When comparing the spectra in Fig. 3 and 4, the number of molecules of azobenzene that are actually involved has to be considered. At first sight, it would appear that the changes in absorbance measured (Fig. 4) are very small, but it must be realised that the amount of photoisomerisable material involved is also very small. The average size of the nanoparticles was 3.7 nm, which corresponds to cluster containing approximately 2000 atoms and a total number of attached ligands of $\sim$280.[39] The total concentration of clusters was 7.2×10^{-9} M, calculated with the measured molar absorption coefficient of $\sim$7910 M^{-1} cm^{-1}. The molar absorption coefficient was determined by measuring the absorbance of the nanoparticle solution for a known silver concentration. Thus, the total concentration of AZO1 available *i.e.*, attached to the nanoparticles, was 2.0 μM for the unlikely condition of full coverage by AZO1. From data in Fig. 3 the change in molar absorption coefficient of AZO2 for the *trans–cis* transformation at 334 nm was 3.17×10^4 M^{-1} cm^{-1}, which is very close to the values observed earlier for *para*-substituted azobenzene derivatives.[40] For full coverage, the change at 348 nm would be $3.17 \times 10^4 \times 2.0 \times 10^{-6} = 0.064$ absorbance units. Therefore, the change observed at this wavelength (Fig. 4) can be accounted for by a 19% exchange of the thiol by AZO1. These are approximate estimates but clearly demonstrate that, since there is no free azobenzene derivative present in the solution, the absorbance changes observed in Fig. 4 are consistent with the amount of attached azobenzene. Therefore, these changes are not small when the concentration of the bound azobenzene is factored in.

Isomerisation of AZO2 aggregates

Fig. 5 shows the spectrum of silver nanoparticles and free AZO2 in *trans* form immediately after adding Ag nanoparticles to the AZO2 solution ($t = 0$). After 30 min of reaction the spectral changes show an increase of absorbance in a wide wavelength range. The difference spectrum (dotted line) shows that the absorbance enhancement has a maximum near 460 nm, which can be correlated to the plasmon band of the nanoparticles. No shift of the plasmon band is seen, implying

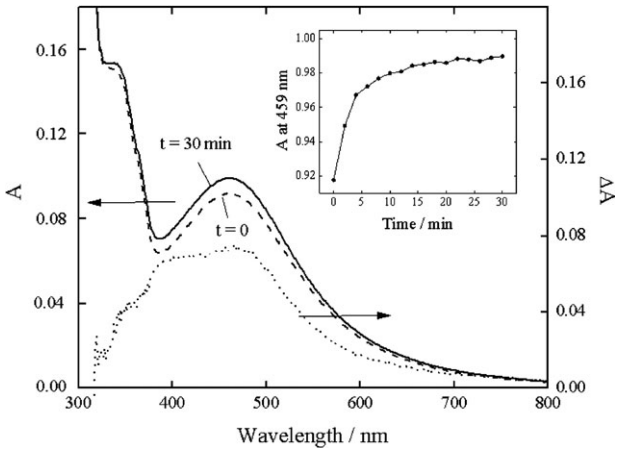

Fig. 5 UV-spectrum of the nanoparticles (solid line) and the formed *trans* AZO2 linked nanoparticle clusters after 30 min of reaction (dashed line). The lowest curve (dotted line) is the difference between these spectra. Inset: Evolution of the absorbance at 459 nm.

none or weak coupling between the nanoparticles' plasmons, when attached to each other by the *trans* conformer of AZO2. The inset of Fig. 5 shows the increase of absorbance at 459 nm as a function of time. It is observed that the absorbance stabilizes after 30 min. Thus, the attachment of the *trans* conformer of the azobenzene group to the surface of a silver nanoparticle induces an enhancement of the plasmon band of the nanoparticle. As discussed previously, this can be a consequence of efficient energy transfer between the chromophore and the nanoparticles. The effect of the change in the polarity of the capping ligand as AZO2 binds to the surface by exchange with the alkane thiol is considered negligibly small. In addition, the amount of exchanged AZO2 compared to the amount of dodecanethiol present on the surface is small in the time scale of 30 min.

Isomerisation of the linker to the *cis* form did not lead to significant differences with the spectrum of free AZO2 (results not shown). Thus, it appears that the conformation of the linker in the nanoparticle aggregates linked with *trans*-AZO2 cannot be changed by photoisomerisation. This is probably due to the formation of rigid, ordered cross-linked structures with the linear *trans*-molecule. Similar inhibition of the *trans–cis* isomerisation has been observed in ordered self-assembling monolayers.[13]

Fig. 6 shows the spectral changes for nanoparticles linked initially with the *cis* conformer of AZO2. Fig. 6A (bottom spectra) shows the initial spectrum of Ag nanoparticles immediately after addition of the dithiol linker ($t = 0$) and the spectrum after allowing the system to react resulting in the formation of aggregates ($t = 60$ min). During this transformation the solution was kept under irradiation of 366 nm light to ensure that the azobenzene moiety was kept in the *cis* conformation. The spectrum of the free AZO2 was subtracted from these measured spectra to allow the observation of changes related only to the coupling of the nanoparticles plasmon band and not to changes related to AZO2. Details of the difference spectra *i.e.*, the difference between the spectrum of nanoparticles in solution ($t = 0$) and that after allowing linking of nanoparticles with the azobenzene dithiol

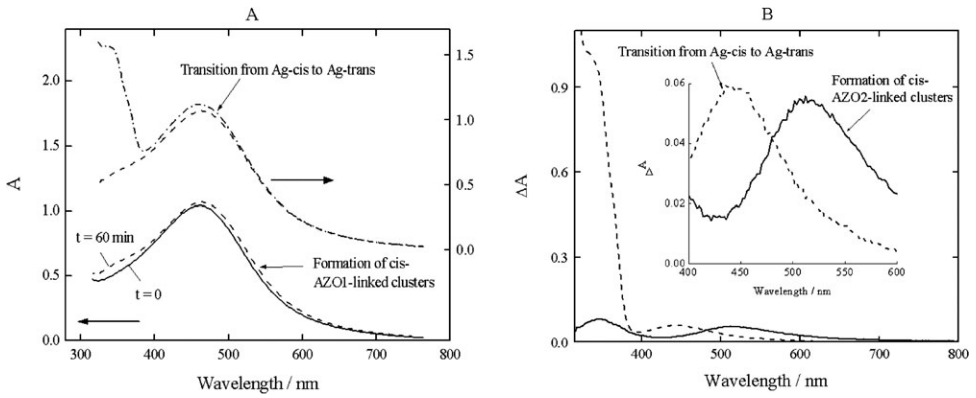

Fig. 6 (A) UV-spectrum of the nanoparticles (solid line) and the *cis* AZO2 linked nanoparticle clusters formed after 60 min (dashed line). The upper spectra repeat the spectrum of *cis* AZO2 linked aggregates and show the spectrum of the aggregates after the linker is isomerised to the *trans* conformation (dash–dot line). For clarity, the second set of spectra is shifted by 0.7 absorbance units. (B) Difference spectra between the AZO2 linked nanoparticle clusters and individual nanoparticles (solid line) and between *trans* AZO2 and *cis* AZO2 linked particle clusters (dashed line). The silver : dithiol ratio was 4.6. The inset shows the detail of the Ag plasmon band spectral region.

in its *cis*-form to occur, are shown in Fig. 6B. The appearance of a well-defined new band at $\sim$510 nm can be observed. Importantly, no absorbance is observed for the azobenzene compound used in this wavelength region. It is proposed that the shift in the position of the plasmon band of $\sim$50 nm is due to the coupling of plasmons of the metal nanoparticles brought close to each other by the linker molecules.

Fig. 6A also shows the change in absorbance brought about by irradiating the above solution containing nanoparticle aggregates (azobenzene as the *cis*-conformer) with 436 nm light, in the expectation that this would change the separation between linked nanoparticles by effecting the *cis*- $\rightarrow$ *trans*-isomerisation reaction. As can be seen, the characteristic absorbance of the *trans*-isomer for $\lambda < 400$ nm is observed. In addition, there is a clear shift in both absorbance intensity and position of the silver plasmon band when the *cis*- $\rightarrow$ *trans*-transformation occurs. Details of the difference in spectra are shown in Fig. 6B.

When analysing the spectral changes that take place on the *cis*–*trans* isomerisation of the AZO2-Ag nanoparticles in solution (Fig. 6), it must be recognised that these result from three contributions. The first, which is the aim of this work, is the changes in the longitudinal coupled plasmons resulting from the expected increase in separation between nanoparticles when the linker changes from the *cis* to the *trans* form. The second change that needs considering results from the initial presence of free AZO2 in solution. The experiment had to be carried out in the presence of free AZO2 in order to ensure the formation of a sufficient amount of aggregates. Although this introduces additional spectral features, it greatly increases the effects observed when increasing the linker concentration, as shown in Fig. 7A and B. The question that needs discussion is whether these spectral changes are due to plasmon changes in the aggregates or result from the azobenzene compound itself. The third change in the spectrum is due to the isomerisation of the AZO2 molecules attached to the nanoparticles.

As shown in Fig. 3 and 4, absorbance changes during isomerisation of the free azobenzene group and azobenzene bound to a silver nanoparticle take place near 440 and 460 nm, respectively. Absorbance changes below 400 nm are more complex to analyze since these refer to electronic transition in the linker molecules and they are not important for the present work that considers coupling of plasmons. The overlapping of the above changes complicates the analysis of the changes in the spectra of AZO2-linked nanoparticles (upper spectra in Fig. 6A). In the difference spectrum (dashed line in Fig. 6B) there is a clear increase observed in absorbance near 440 nm. A quantitative analysis of this difference spectrum is not possible from the measurements performed. However, a comparison between the difference spectrum in Fig. 4, where a surface coverage of AZO1 of 19% is achieved and the difference spectrum of Fig. 5, where a very low surface coverage is present, shows that the contributions brought about by the isomerisation are of the same order of magnitude ($\sim$5% decrease in the plasmon band) compared to the enhancement of the plasmon band when *trans* AZO2 is attached to the nanoparticle ($\sim$7% increase in the plasmon band). Thus, it is very likely that, with low surface coverage, the latter contribution is stronger and obscures the first one.

It was expected that the difference spectrum between the *trans*- and *cis*-AZO2-linked nanoparticles would show a negative change in absorbance at 510 nm as the longitudinal plasmon band would shift to smaller wavelengths. No negative change was observed, but the increase in absorbance at 440 nm in Fig. 6B can be considered as a sum of a positive contribution explained above and a negative contribution due to the change in the coupled plasmon band. For the above discussed reasons, an accurate value for the shift of the plasmon resonance for aggregates linked with *trans* AZO2 can not be quantified.

Fig. 7 shows the same experiment as in Fig. 6, but with a higher AZO2 concentration. The positions of the initial and final plasmon bands are the same in both experiments, but a red-shift of the plasmon band of the *cis*-AZO2-linked nanoparticles is seen in Fig. 7. This can be explained by the increased intensity of the longitudinal plasmon band due to the increased number of aggregates formed. The positions of the measured plasmon bands are listed in Table 1.

Considering these findings, the isomerisation from *cis* to *trans* with 436 nm light shifted the longitudinal plasmon band

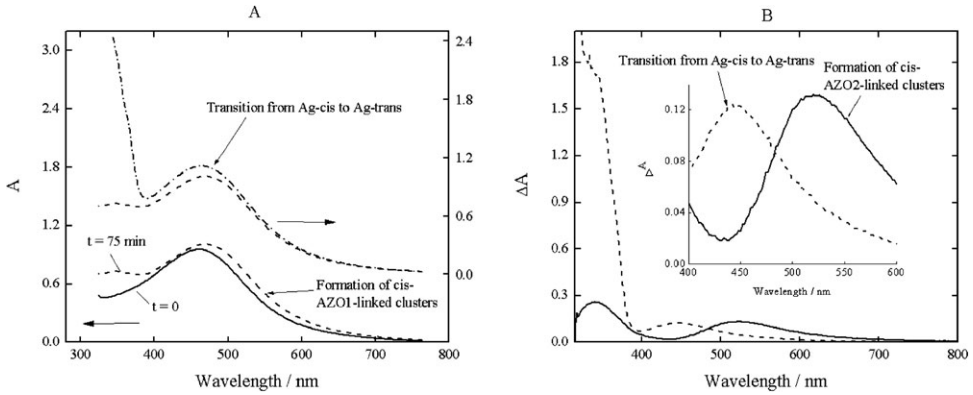

Fig. 7 (A) UV-spectrum of the nanoparticles (solid line) and the *cis* AZO2 linked nanoparticle clusters formed after 75 min (dashed line). The upper spectra repeat the spectrum of *cis* AZO2 linked aggregates and show the spectrum of the aggregates after the linker is isomerised to the *trans* conformation (dash–dot line). For clarity, the second set of spectra is shifted by 0.7 absorbance units. (B) Difference spectra between the AZO2 linked nanoaparticle clusters and individual nanoparticles (solid line) and between *trans* AZO2 and *cis* AZO2 linked particle clusters (dashed line). The silver : dithiol ratio was 1.8. The inset shows the detail of the Ag plasmon band spectral region.

from 510 nm towards smaller wavelengths, a consequence of the increasing distance between the particles. The peak separations can be compared with earlier results for gold nanoparticles from Rechberger *et al.*[26] and from Sendroiu *et al.*[41] where a dependence between the position of the coupled longitudinal plasmon band and the distance between nanoparticles was determined. The dependence is universal, thus the plasmon coupling of nanoparticles of different sizes can be compared by expressing the separation in a dimensionless form. For the 3.7 nm particles, the dimensionless parameter distance/diameter, *i.e.* the ratio between the center to center separation and the particle diameter, is approximately 1.2 for the *cis* isomer and 1.5 for the *trans* isomer of AZO2. The length of the molecule was estimated from a simple molecular model (ChemSketch) to be 17 Å for the *trans* conformer and 14 Å for the *cis* conformer. The particle separation was estimated by assuming perpendicular ligand orientation. In the next section, an approximation for the distance between the particles is calculated based on the above linker lengths and the measured shift of the plasmon band.

It can be concluded that photoreactive linkers can be used to control the interaction between optically excited plasmons of nanoparticles, thus displaying a photoswitchable behavior.

Model of a nanoparticle pair

In what follows, a simple analysis of the expected changes due to linker photoisomerisation is presented. The analysis is based on the observation that the spectra of solution of aggregated nanoparticles can be deconvoluted into two plasmon band contributions.[41] The distance dependence of the longitudinal plasmon contribution indicated that only nearest neighbor interactions need to be considered. The optical spectrum of two attached nanoparticles was calculated using a simplified model describing the coupling of plasmon resonances of two clusters in close proximity.[43,44] This model takes into account the changes in the local field near the neighbouring clusters due the irradiation by light. It is assumed that no tunneling of electrons occurs between the clusters *i.e.* the clusters remain electrically isolated in the aggregates. Since only cluster pairs are considered and the clusters are small in diameter d ($d \ll \lambda$), the fluctuation of the electromagnetic field due to the presence of nanoparticles can be neglected. This is called the quasi-static approximation[41] and it simplifies the mathematical treatment of the problem.

Table 1 The positions of the measured plasmon bands

	Plasmon band/nm [a]	Plasmon band/nm [b]	Plasmon band (nm)[c]
Individual MPCs	459	462	461
MPCs linked with *cis*-AZO2	—	465	472
MPCs linked with *trans*-AZO2	458	460	461

[a] Ag : dithiol = 4.6, AZO2 initially in *trans* conformation. [b] Ag : dithiol = 4.6, AZO2 initially in *cis* conformation. [c] Ag : dithiol = 1.8. AZO2 initially in *cis* conformation.

The dependence of the complex dielectric function of the silver nanoparticles on size was included by replacing the bulk relaxation constant Γ_∞ in the Drude dielectric function by a radius dependent quantity as follows:[44]

$$\varepsilon(\omega, R) = \varepsilon_{\text{bulk}}(\omega) + \omega_p^2\left(\frac{1}{\omega^2 + \Gamma_\infty^2} - \frac{1}{\omega^2 + \Gamma(R)^2}\right) + i\frac{\omega_p^2}{\omega}\left(\frac{\Gamma(R)}{\omega^2 + \Gamma(R)^2} - \frac{\Gamma_\infty}{\omega^2 + \Gamma_\infty^2}\right) \quad (1)$$

where

$$\Gamma(R) = \Gamma_\infty + A\frac{v_F}{R} \quad (2)$$

and

$$\Gamma_\infty = \frac{v_F}{l_\infty} \quad (3)$$

ω is the radial frequency, R is the radius of a nanoparticle, ω_p is the plasmon frequency of silver, v_F is the Fermi velocity of silver and l_∞ is the mean free path in bulk silver. Since the radius of the particles investigated here is smaller than the mean free path in the bulk metal, the particle radius has been

taken as the mean free path to calculate the dielectric function of the particles. A is a shape-dependent factor and can be taken as 1 for spherical particles.[44] The dielectric function for bulk silver was calculated from optical constants obtained from Quinten.[45] The bulk plasma frequency was calculated from:[46]

$$\omega_p = \sqrt{\frac{Ne^2}{\varepsilon_0 m_e}} \quad (4)$$

where N is the density of electrons, e is the elementary charge, ε_0 is the permittivity of free space and m_e is the effective mass of an electron, which is taken as $0.96 \times m_0$ [42] (m_0 = the mass of the electron).

The polarisability of nanoparticle pairs was calculated from the polarisabilities of single particles.[44] The model considers that the broadening of the plasmon absorption peak is due to two separate resonances appearing from the electromagnetic interaction between two particles close to each other. Considering only the transversal and longitudinal in-phase modes the component of the polarisability parallel to the external field ($\alpha_{\|}$) of a pair consisting of two particles of equal size is given by:

$$\langle \alpha_{\|\text{pair}} \rangle = \frac{2C\varepsilon_m \eta}{3}\left(\frac{1}{1+\eta\Gamma_-} + \frac{2}{1+\eta\Gamma_+}\right) \quad (5)$$

where

$$C = 4\pi\varepsilon_0 R^3 \quad (6)$$

$$\eta = \frac{\varepsilon(\omega, R) - \varepsilon_m}{\varepsilon(\omega, R) + 2\varepsilon_m} \quad (7)$$

and

$$V^2 = \left(\frac{R}{l}\right)^6 \quad (8)$$

ε_m is the dielectric permittivity of the embedding medium, $\Gamma_\pm$ are the eigenvalues of the aggregate modes, and l is the center-to-center distance between the particles.

Under quasi-static conditions, the extinction cross-section C_{ext} and scattering cross-section C_{sca} can be calculated from the polarisability α of an individual nanoparticle as follows:[41]

$$C_{ext} = K\text{Im}\{\alpha\} \quad (9)$$

$$C_{sca} = \frac{K^4}{6\pi}|\alpha|^2 \quad (10)$$

with

$$K = 2\pi n_m \quad (11)$$

where n_m is the refractive index of the embedding medium, the square root of ε_m. The absorption cross-section C_{abs} is the difference between extinction and scattering cross-section.

The distance between the metal cores was calculated based on the measured shift of the coupled plasmon band, of approximately 50 nm. The theoretical value for the particle–particle separation of the *cis*-AZO2-linked nanoparticles was ~4 Å, which corresponds a value of ~1.1 for the distance/diameter ratio. The approximate particle separations and spectral shifts and those calculated with the above model are compared in Table 2. Because the calculations were carried out for bare silver particles, the absolute peak width and wavelength are not in very good agreement with the measured spectra. Despite this, the separation between the two absorption bands arising from the coupled plasmons of the particle pairs are reasonably close to the measured values.

Table 2 Estimated and calculated particle separations and shifts of the plasmon resonances

	Particle separation/ Å [a]	Particle separation/ Å [b]	Shift of the plasmon band/ nm [c]	Shift of the plasmon band/ nm [d]
MPCs linked with *cis*-AZO2	6.8	4.0	36	50
MPCs linked with *trans*-AZO2	17	—	17	—

[a] Approximated from a molecular model. [b] Calculated from the measured spectral shift. [c] Calculated from the approximated particle separations. [d] Measured.

There are several reasons why the measured and calculated values are not in agreement. The MPCs are capped with dodecanethiol that provides an additional dielectric layer at the particles surface that has to be taken into account in a more detailed model.[46,47] There might also be some steric hindrance inhibiting the full conformational changes of the azobenzene moiety inside a thiol monolayer and some degree of interdigitation could be required for the nanoparticles to reach the distance of closest approach predicted by the dimensions of the linker in the two conformations. The structures of systems consisting of ideal bare particles and more realistic particles capped with dielectric material are compared in Fig. 8.

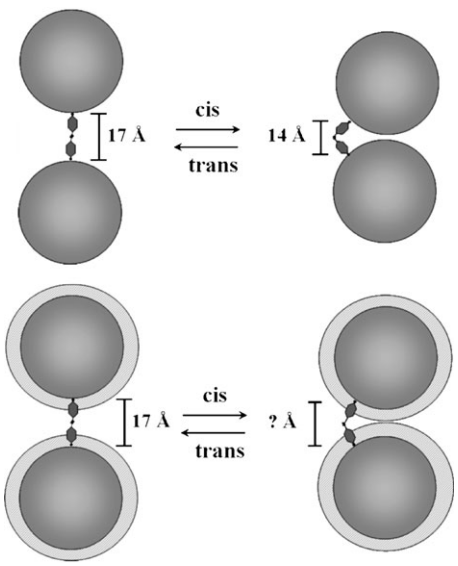

Fig. 8 Schematic diagram of the dithiol linked nanoparticle pair system studied. The figure at the top corresponds to the ideal bare particles case described by the model. The lower figure represents the case where a layer of adsorbed thiol is present on the particles surface, which hinders the approach of the particles.

Sidhaye *et al*.[6] have shown earlier that the range of movement in a nanoparticle network cross-linked with isomerizable molecules is highly dependent on the properties of the capping agent, in agreement with the present results.

In spite of these uncertainties the importance of the present work is to have demonstrated that switching of different properties of coupled plasmon between nanoparticles can be achieved by the use of photoresponsive linkers. Of particular relevance is the possibility of controlling the optical properties of nanoparticle architectures with light of a different wavelength from that corresponding to the plasmon resonance frequency.

Conclusions

The photoisomerisation and spectral properties of silver nanoclusters derivatised with azobenzene functionalised thiols have been studied. It is shown that the matching of the plasmon resonance of the silver particles with the absorption band of *cis*-azobenzene results in interaction between the plasmon band and the azobenzene chromophore. The study of energy transfer between the two species requires further investigation.

Electromagnetic coupling of dithiol-linked silver nanoparticle aggregates was observed as a red-shift in the measured UV-Vis spectra. This red shift could be controlled by changing the interparticle distance by photoisomerisation between the *trans* and *cis* states of the azobenzene linker dithiol. The measured changes were compared with theoretical calculations for bare silver nanoparticles. The observed shift between the original plasmon band and the new band due to the coupling between the nanoparticles was close to that predicted from the model and earlier experimental work.

The importance of this work is to have shown that changing the separation between nanoparticles by photoisomerisation of a photoreactive linker results in measurable changes in the coupling of the particles plasmons. The effect is not very large for the conditions investigated but optimisation of conditions could result in practical applications for these photoswitchable plasmonic systems.

Acknowledgements

The authors acknowledge Kemira Foundation, Finland, for supporting this work.

References

1 J. P. Novak, L. C. Brousseau III, F. W. Vance, R. C. Johnson, I. Buford Lemon, J. T. Hupp and D. L. Feldheim, *J. Am. Chem. Soc*., 2000, **122**, 12029.
2 D. I. Gittins, D. Bethell, R. J. Nichols and D. J. Schiffrin, *Adv. Mater*., 1999, **11**, 737.
3 C. R. Mayer, S. Neveu and V. Cabuil, *Adv. Mater*., 2002, **14**, 595.
4 W. Haiss, R. J. Nichols, S. J. Higgins, D. Bethell, H. Höbenreich and D. J. Schiffrin, *Faraday Discuss*., 2004, **125**, 179.
5 A. Pucci, N. Tirelli, E. A. Willneff, S. L. M. Schroeder, F. Galembecke and G. Ruggeri, *J. Mater. Chem*., 2004, **14**, 3495.
6 D. S. Sidhaye, S. Kashyap, M. Sastry, S. Hotha and B. L. V. Prasad, *Langmuir*, 2005, **21**, 7979.
7 R. Mikami, M. Taguchi, K. Yamada, K. Suzuki, O. Sato and Y. Einaga, *Angew. Chem., Int. Ed*., 2004, **43**, 6135.
8 M. Alvaro, M. Benitez, D. Das, H. Garcia and E. Peris, *Chem. Mater*., 2005, **17**, 4958.
9 Y. Einaga, *Bull. Chem. Soc. Jpn*., 2006, **79**, 361.
10 F. Callari, S. Petralia and S. Sortino, *Chem. Commun*., 2006, 1009.
11 G. Zimmerman, L.-Y. Chow and U. J. Paik, *J. Am. Chem. Soc*., 1958, **80**, 3528.
12 T. Schultz, J. Quenneville, B. Levine, A. Toniolo, T. J. Martinez, S. Lochbrunner, M. Schmitt, J. P. Shaffer, Z. Zgierski and A. Stolow, *J. Am. Chem. Soc*., 2003, **125**, 8098.
13 S. D. Evans, S. R. Johnson, H. Ringsdorf, L. M. Williams and H. Wolf, *Langmuir*, 1998, **14**, 6436.
14 M. Irie, Y. Hirano, S. Hashimoto and K. Hayashi, *Macromolecules*, 1981, **14**, 262.
15 M. Kamenjicki, I. K. Lednev and S. A. Asher, *J. Phys. Chem. B*, 2004, **108**, 12637.
16 A. Archut, F. Vogtle, L. De Cola, G. C. Azzellini, V. Balzani, P. S. Ramanujam and R. H. Berg, *Chem.–Eur. J*., 1998, **4**, 699.
17 D. S. Sidhaye, S. Kashyap, M. Sastry, S. Hotha and B. L. V. Prasad, *Langmuir*, 2005, **21**, 7979.
18 B. V. Shankar and A. Patnaik, *Langmuir*, 2006, asap.
19 H. Akiyama, K. Tamada, J. Nagasawa, K. Abe and T. Tamaki, *J. Phys. Chem. B*, 2003, **107**, 130.
20 A. Manna, P.-L. Chen, H. Akiyama, T.-X. Wei, K. Tamada and W. Knoll, *Chem. Mater*., 2003, **15**, 20.
21 R. Wang, T. Iyoda, T. A. Tryk, K. Hashimoto and A. Fujishima, *Langmuir*, 1997, **13**, 4644.
22 C. Guarise, L. Pasquato and P. Scrimin, *Langmuir*, 2005, **21**, 5537.
23 J. P. Novak, L. C. Brousseau, III, F. W. Vance, R. C. Johnson Lemon, I. Buford, J. T. Hupp and D. L. Feldheim, *J. Am. Chem. Soc*., 2000, **122**, 12029.
24 I. Hussain, Z. Wang, A. I. Cooper and M. Brust, *Langmuir*, 2006, **22**, 2938.
25 P. Ahonen, T. Laaksonen, A. Nykänen, J. Ruokolainen and K. Kontturi, *J. Phys. Chem. B*, 2006, **110**, 12954.
26 W. Rechberger, A. Hohenau, A. Leitner, J. R. Krenn, B. Lamprecht and F. R. Aussenegg, *Opt. Commun*., 2003, **220**, 137.
27 S. Y. Park, J.-S. Lee, D. Georganopoulou, C. A. Mirkin and G. C. Schatz, *J. Phys. Chem. B*, 2006, **110**, 12673.
28 M. J. Hostetler, S. J. Green, J. J. Stokes and R. W. Murray, *J. Am. Chem. Soc*., 1996, **118**, 4212.
29 W. Caseri, *Macromol. Rapid Commun*., 2000, **21**, 705.
30 M. Brust, M. Walker, D. Bethell, D. J. Schiffrin and R. J. Whyman, *Chem. Soc., Chem. Comm*., 1994, 801.
31 M. M. Oliveira, D. Ugarte, D. Zanchet and A. J. G. Zarbin, *J Coll. Int. Sci*., 2005, **292**, 429.
32 W. Rasband, National Institutes of Health, USA, http://rsb.info.nih.gov/ij/.
33 L. Cai, Y. Yao, J. Yang, D. W. Price Jr and J. M. Tour, *Chem. Mater*. , 2002, **14**, 2905.
34 W. W. Simons, *The Sadtler Handbook of Ultraviolet Spectra*, Sadtler, 1979.
35 Z. Pan, L. J. Wang and Rothbereg, *J. Phys. Chem. B*, 2006, **110**, 17383.
36 K. G. Thomas and P. V. Kamat, *Acc. Chem. Res*., 2003, **36**, 888.
37 A. M. Glass, P. F. Liao, J. G. Bergman and D. H. Olson, *Opt. Lett*., 1980, **5**, 368.
38 S. Pan and L. J. Rothberg, *J. Am. Chem. Soc*., 2005, **127**, 6087.
39 M. J. Hostetler, J. E. Wingate, C.-J. Zhong, J. E. Harris, R. W. Vachet, M. R. Clark, J. D. Londono, S. J. Green, J. J. Stokes, G. D. Wignall, G. L. Glish, M. D. Porter, N. D. Evans and R. W. Murray, *Langmuir*, 1998, **14**, 17.
40 C. Ruslim and K. Ichimura, *J. Mater. Chem*., 2000, **10**, 2704.
41 I. E. Sendroiu, S. F. L. Mertens and D. Schiffrin, *Phys. Chem. Chem. Phys*., 2006, **8**, 1430.
42 P. B. Johnson and R. Christy, *Phys. Rev. B: Solid State*, 1972, **6**, 4370.
43 C. F. Bohren and D. R. Huffman, *Absorption and Scattering of Light by Small Particles*, John Wiley, New York, 1983.
44 U. Kreibig and M. Vollmer, *Optical Properties of Metal Clusters*, Springer, New York, 1995, p. 159.
45 M. Quinten, *Z. Phys. B: Condens. Matter*, 1996, **101**, 211.
46 P. Mulvaney, *Langmuir*, 1996, **12**, 788.
47 A. Pinchuk, U. Kreibig and A. Hilger, *Surf. Sci*., 2004, **557**, 269.

